Korean J. Chem. Eng., 34(3), 844-853 (2017)
DOI: 10.1007/s11814-016-0307-z

pISSN: 0256-1115
eISSN: 1975-7220

Quantitative estimation of internal concentration polarization in a spiral wound forward osmosis membrane module compared to a flat sheet membrane module

Changseong Bae‡, Kiho Park‡, Hwan Heo, and Dae Ryook Yang†

Department of Chemical and Biological Engineering, Korea University, 145, Anam-ro, Seongbuk-gu, Seoul 02841, Korea
(*Received 12 August 2016 • accepted 30 October 2016*)

Abstract−Internal concentration polarization (ICP) within the forward osmosis (FO) membrane affects the reduction of driving force. The magnitude of ICP in the FO membrane was investigated experimentally by measuring water flux in both spiral wound (SW) and flat-sheet (FS) modules with different draw solutions (sodium chloride, sodium sulfate, and disodium phosphate). The FO SW module always shows inferior water flux performance to the FO FS module. The water flux in the FO SW module can be easily estimated by just changing structure parameter. The estimated structure parameter in the FO SW module is 9.1325×10^{-4} m, which is quite higher than 4.2×10^{-4} m in the FO FS module. The increase of the structure parameter is attributed to the bending of the FO membrane in the SW module. It can be concluded that a module design such like SW type is not suitable for the FO process.

Keywords: Forward Osmosis, Internal Concentration Polarization, Spiral Wound Membrane Module, Parameter Estimation, Desalination

INTRODUCTION

Forward osmosis (FO) is a phenomenon in which water molecules in a solution of low concentration (feed solution) migrate into a more concentrated solution (draw solution) by diffusion across a semipermeable membrane. The driving force for FO is the osmotic pressure difference corresponding to the concentration difference between two solutions (draw and feed solution) facing a semipermeable membrane. FO has several advantages, such as low energy consumption due to its spontaneity, and low fouling propensity compared to a pressure-driven membrane process. Thus, FO has received growing attention in research and industrial fields [1]. Up to now, FO has been applied in various ways such as seawater desalination [2-5], waste water treatment [6-8], power generation by pressure retarded osmosis (PRO) [9-11], and pharmaceutical processing [12,13].

Internal concentration polarization (ICP) is a phenomenon by which the osmotic pressure of draw and feed solutions within the membrane porous support layer is decreased or increased by the migrating permeate water flow from feed solution to draw solution. To be specific, water from feed solution facing the active rejection layer (AL-FS mode) migrates into draw solution across the membrane, the draw solution becomes diluted, and the diluted solution is rarely stirred within the support layer. On the other hand, water from feed solution facing the porous support layer (AL-DS mode) migrates into draw solution across the membrane, the feed solution becomes concentrated, and the concentrated solution is rarely stirred within the support layer. Therefore, the effective osmotic pressure and water flux decrease. ICP reduces water flux through the membrane significantly, and it has been one of the main issues of the FO process [14-17].

The FO membrane intrinsic properties could be expressed as the water permeability (A), the salt permeability (B), and the membrane structure (S) parameter [18]. Separation performance of each FO membrane can be quantified with these parameters. Especially, the S parameter is determined by the membrane porous support layer thickness, the porosity, and the tortuosity [16,18-20]. When the membrane porous support layer thickness and tortuosity become larger and the porosity becomes smaller, the S parameter becomes larger. Since a large S parameter causes significant ICP in FO membrane, the effective osmotic pressure difference is reduced extremely compared to FO membrane with small S parameter [21-25]. Therefore, to quantify the water flux in FO process, it is very important to know not only A, B parameters but also S parameter in FO membrane as precisely as possible.

To operate a membrane process, membranes must be loaded into membrane modules. Flat sheet (FS) membrane modules have been used for laboratory-scale operations [1]. The active rejection area of an FS module is approximately below 0.01 m^2. Since the structure of an FS module is very simple, it is suitable for a study of the characteristics of the membrane itself. Spiral wound (SW) membrane modules have been used for large-scale operations [1]. The active rejection area of SW module is approximately 3-8 m^2 [26,27]. SW module is suitable for a study of the whole membrane process combining subsequent processes such as the recovery and reconcentration of draw solution and also a study of its optimization [1, 27]. A majority of previous studies for FO membrane have been conducted with FS modules [4,16,28-30]. Several researches for FO membrane in SW modules have also been done recently to investi-

†To whom correspondence should be addressed.
E-mail: dryang@korea.ac.kr
‡These authors contributed equally to this work.
‡This article is dedicated to Prof. Sung Hyun Kim on the occasion of his retirement from Korea University.

gate the actual performance of water flux in industrial scale [26,27, 31,32]. The difference of water flux between FS and SW modules has been compared in these researches. However, the quantification of ICP effect in both FO membrane modules has not been investigated. The water flux values and the ICP effects even with the same FO membranes can be totally different in accordance with the various complex factors when different types of membrane modules are applied to membranes. Therefore, the analysis and comparison should be conducted at different types of membrane modules.

We investigated the magnitude of the ICP in the FO membrane by experiments with commercially available SW and FS modules, and a simulation model for estimation of the water flux in the FO SW module was developed. The experimental results in the FO SW module were examined with the simulation results from the newly estimated structure parameter. The estimated structure parameter describes the magnitude of the ICP in the FO SW membrane module. The estimated structure parameter and the developed model were verified by the experimental data from different draw solutions (Na_2SO_4 and Na_2HPO_4). In addition, it was demonstrated why the structure parameter is changed in the FO SW module comparing to the FO FS module.

MATERIALS AND METHODS

1. FO Spiral Wound Membrane Module

SW4040MS FO membrane module (Hydration Technology Innovations, U.S.) was used for the FO experiments and the membrane was made of cellulose triacetate (CTA). The FO SW membrane module was loaded onto Champ 4040 tubular pressure vessel (AXEON water technologies, U.S.). The vessel was made of polyvinyl chloride (PVC), and had four ports at two inlets and two outlets. Even though the FO SW membrane module was designed by referring to reverse osmosis (RO) SW membrane module, the detailed design is quite different. Fig. 1 shows schematic representations and cross-sectional views of each FO and RO SW membrane module for comparison. Since the FO process requires two inlet solutions (feed and draw solutions), the design of the FO SW membrane module should be considered for FO membrane to be placed between feed and draw solutions as much as possible in the SW module. Thus, the flow path of one inlet solution was designed for bypassing the inside membrane envelope with centered glue line. On the other hand, the other inlet solution is pumped into the outer space between membrane envelope to face the bypassing inlet

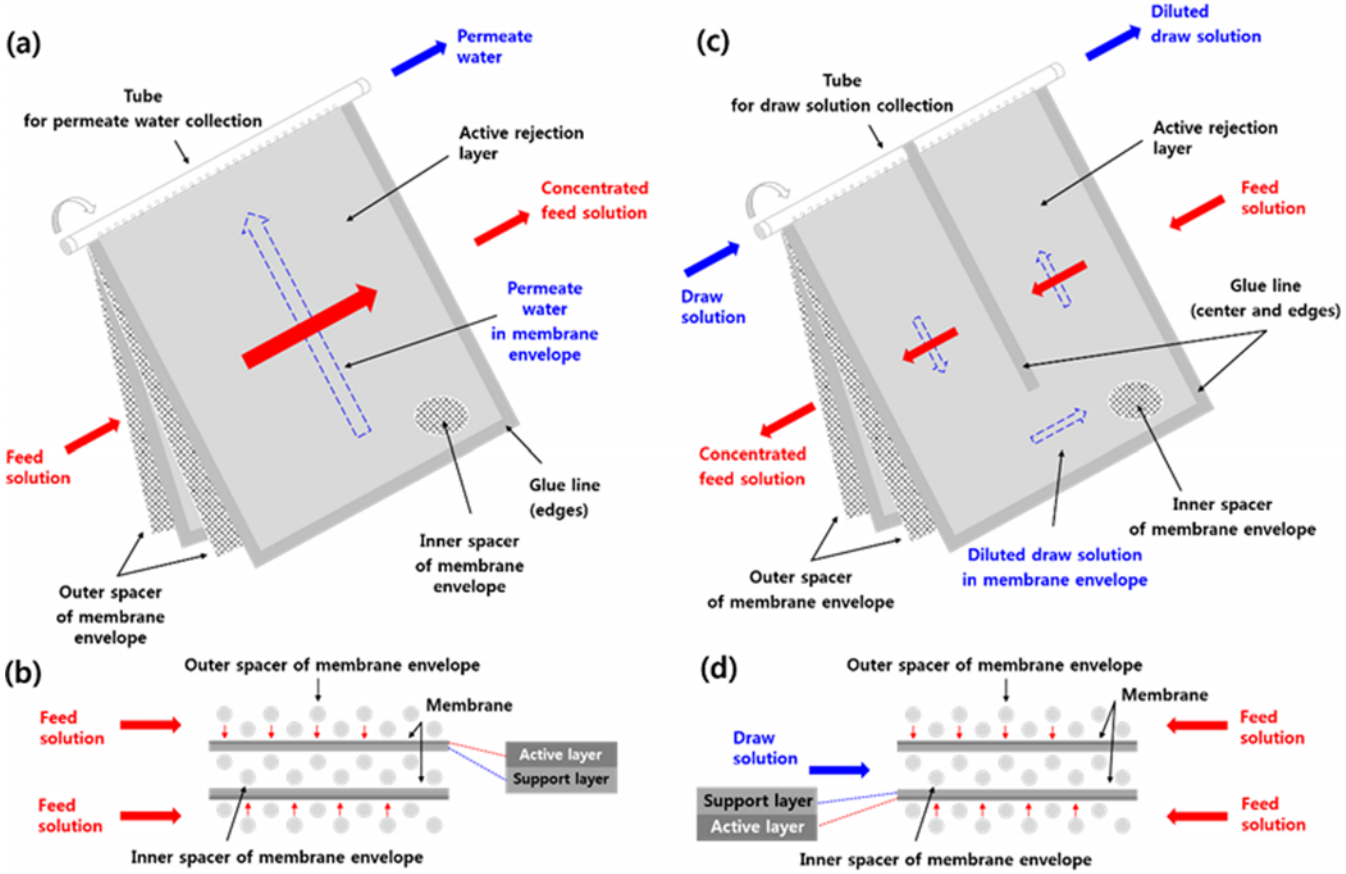

Fig. 1. (a) A schematic representation of RO spiral wound module with feed solution. Spacers are positioned both inside and outside of the membrane envelopes. (b) A cross-sectional view of the RO membrane envelope. The active rejection layer faces the feed solution on the outside of the membrane envelope. (c) A schematic representation of FO spiral wound module with feed and draw solution in counter-current. (d) A cross-sectional view of the FO membrane envelope. The active rejection layer faces to the feed solution on the outside of the membrane envelope and the porous support layer faces the draw solution on the inside of the membrane envelope (AL-FS mode).

solution inside the membrane envelope across the FO membrane. However, the packing density of the FO SW module is significantly reduced due to its complex constitution. It causes a reduction of active rejection area in FO SW module compared to RO SW module. The active rejection area of FO SW module is 3.2 m^2 and that of RO SW module is 7.4 m^2 [27]. FO SW module can be operated with two different types of membrane orientations, AL-FS mode and AL-DS mode. These operation modes can be changed by which solution is fed into the inlet central tube line described in Fig. 1. In this module, when draw solution is fed into the inlet central tube line, and feed solution into the spacers between rolled membrane envelope, this type of module operation is referred to as AL-FS mode.

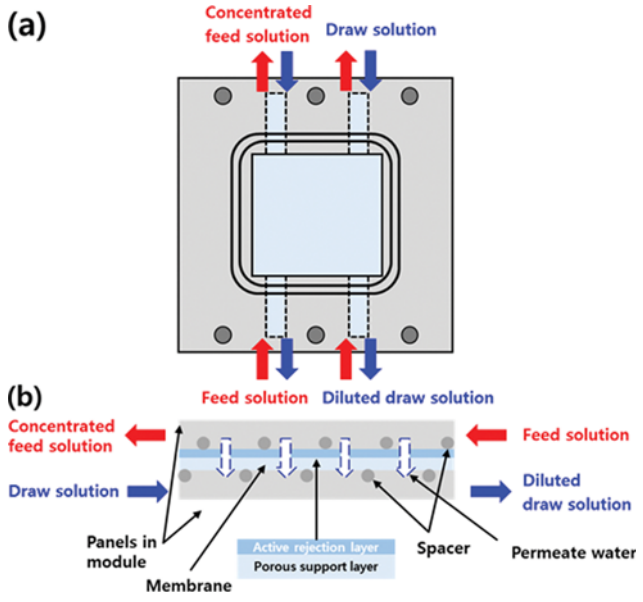

Fig. 2. (a) A schematic representation of the FO flat sheet module with feed and draw solution. Spacers are positioned on the active rejection layer and the porous support layer of the membrane. (b) A cross-sectional view of the FO flat sheet module. The active rejection layer faces the feed solution (AL-FS mode).

2. FO Flat Sheet Membrane Module

An FO FS membrane module manufactured of acrylic panels was used for the FO experiments and the FO membrane was made of CTA, which is the same material as the FO SW module. Fig. 2 shows an illustration and flow path of feed and draw solution in the membrane module. Like the FO SW module, the flat sheet FO module has two operating modes (AL-FS and AL-DS). Fig. 2 shows a schematic diagram and a cross-sectional view of the flat sheet FO membrane module. The active rejection area of the FO membrane is 9 cm^2.

3. Chemicals

Sodium chloride (NaCl, 99%; Daejung chemicals, Korea) was used for feed and draw solute to investigate water flux performance through the membrane according to operating modes (AL-FS and AL-DS) in the FO SW module. Disodium phosphate (Na_2HPO_4, 99%; Daejung chemicals, Korea) and sodium sulfate (Na_2SO_4, 99%; Daejung chemicals, Korea) were used as draw solutes and NaCl was the feed solute to examine water flux performance through the membrane according to different draw solutes in FO SW and FO FS modules, respectively.

4. Experimental Set-up

Fig. 3(a) and (b) show schematic diagrams of FO SW and FO FS experimental system, respectively. To measure operating variables such as flow rate, pressure, conductivity, and temperature in the FO SW module experimental system, some measuring devices such as flow rate sensors (2536 Roter-X paddlewheel; Signet, U.S.), pressure sensors (12780449 A-10; WIKA, Germany), conductivity sensors (3-2822-1; Signet, U.S.), and temperature transmitters (TSG; Sensys, Korea) were installed in the pipelines and tanks. Circulation pumps (MX-1350-MH; CHEONSEI, Korea) were used. Indicators such as flow rate indicators (8550; Signet, U.S.), pressure indicators (HD-1200-N; HYUNDAI power system, Korea), and conductivity indicators (8860; Signet, U.S.) display the measured variables in real time. The data from the indicators were gathered to the data acquisition hardware (Labjack U12; ezDAQ, Korea). The data acquisition hardware was connected to a programing tool (LabVIEW; National Instruments, U.S.) in a computer, and the programing tool could save and organize the data. Feed and draw solution were recirculated to each tank consistently.

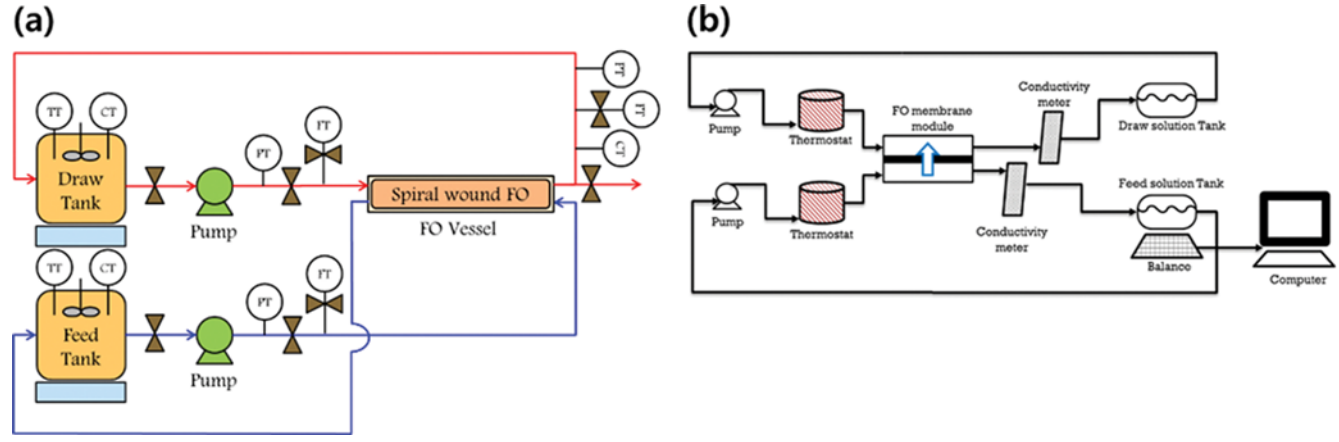

Fig. 3. Schematic diagram of FO experimental system (a) with FO SW module, (b) with FO FS module.

In the FO FS module experimental system, circulation pumps (Masterflex L/S; Cole-Parmer Instrument Company, U.S.) were used. The mass water flux measured from balances (Ranger 7000; OHAUS, U.S.) were collected using programing tools (Balance talk; OHAUS, U.S.) into computers. Temperatures of solutions in each tank were controlled by the jacketed temperature control system with circulators (Lab Companion RW-0525G; Jeio Tech, Korea).

5. Experimental Procedure

Circulation pumps were used for consistent circulation of feed and draw solutions in both FO SW and FO FS modules. The operating pressure was fixed at 1-1.1 bar. The flow rates of feed and draw solutions at the inlet and outlet of the FO SW and FO FS modules were 18.2-18.4 and 8.2-8.4 L/min, and 100 mL/min, respectively. Since the draw solution enters the central tube of the FO SW module and then flows through in the membrane envelope, the flow of the draw solution should overcome more flow resistance than that of the feed solution. Therefore, the flow rate of the draw solution in the FO SW module was set to become smaller than feed flow rate [27]. The operating time was 25 minutes for the FO SW module and 30 minutes for the FO FS module. To examine the effect of operating mode (AL-FS and AL-DS), NaCl with deionized (DI) water was used as draw and feed solution in both FO SW and FO FS module. The concentrations of draw solutions were 0.61, 0.71, 0.81, 1.01, and 1.21 mol/L and feed solution were 0, 0.1, 0.2, 0.4, and 0.6 mol/L. The concentration difference between feed and draw solution was fixed as 0.61 mol/L for investigating how much the magnitude of concentration polarization would be influenced by the concentrations of draw and feed solutions. The operating temperature was 20-21 °C. In addition, to examine the effect of other draw solutions, Na_2SO_4, and Na_2HPO_4 with DI water were used as draw solutions, and NaCl with DI water was used as feed solution in both FO SW and FO FS module. The draw solutes were selected for suitable candidates of hybrid FO, crystallization, and RO hybrid system. The concentration of draw solutions was the saturated solubility of each Na_2SO_4 and Na_2HPO_4 solution at 30 °C, which was 2.46 and 1.27 mol/L, respectively. The concentration of feed solution was 0.61 mol/L, which was selected to mimic the concentration of seawater. The operating temperature was 30-31 °C.

The water flux in the FO SW module was determined by measuring the draw flow rate at the inlet and outlet of the FO SW module and the level difference of the feed and draw solutions in each tank between before and after operation. The water flux in the FO FS module was determined by measuring the weight of feed or draw solutions in each tank. The salt flux in the FO SW and FO FS modules was measured from the conductivity of feed and draw solutions in each solution tank. A portable conductivity meter (YK-2005WA; Lutron Electronic Enterprise, Taiwan) was used in the FO FS module; a conductivity sensor in each tank was used in the FO SW module.

6. Modeling

The water and salt flux through the membrane in the typical FO process can be described as the proportionality of the difference in osmotic pressures between feed and draw solutions as follows [33]:

$$J_w = A(\Delta\pi - \Delta P) \quad (1)$$

$$J_s = B(C_D - C_F) \quad (2)$$

where J_w is the water flux, J_s is the salt flux, $\Delta\pi$ is the difference in bulk solution osmotic pressures, ΔP is the difference in applied pressures, C_D and C_F are the concentration of draw and feed solution, and A, B are the water and salt permeability, respectively. The osmotic pressure can be expressed as the modified van't Hoff equation:

$$\pi = \frac{N_{ion} CRT}{M_w} \quad (3)$$

where N_{ion} is the ionization number in the water, R is the gas constant, C is the concentration of solute, T is the temperature, and M_w is the molecular weight.

Concentration polarization should be considered in membrane process modeling since it is the main reason for decrease in effective osmotic pressure difference across the membrane compared to the bulk osmotic pressure difference. There are two types of concentration polarization, external concentration polarization (ECP) and ICP. The ECP can be expressed as [33]

$$\frac{\pi_{F,m}}{\pi_{F,b}} = \exp\left(\frac{J_w}{k}\right) \quad (4)$$

$$\frac{\pi_{D,m}}{\pi_{D,b}} = \exp\left(-\frac{J_w}{k}\right) \quad (5)$$

$$k = \frac{Sh \cdot D}{d_h} \quad (6)$$

$$Sh = 1.85\left(ReSc\frac{d_h}{L}\right)^{0.33} \text{ (laminar flow)} \quad (7)$$

$$Sh = 0.04Re^{0.75}Sc^{0.33} \text{ (turbulent flow)} \quad (8)$$

where π is the osmotic pressure, subscript F and B is the feed and draw solution, subscript m and b is the membrane surface and bulk solution, respectively, k is the mass transfer resistance, Sh is the Sherwood number, D is the diffusivity, d_h is the hydraulic diameter, Re is the Reynolds number, L is the length of the channel, and Sc is the Schmidt number. The ICP can be also modeled as follows [33]:

$$C_{D,m} = C_{F,m} - \frac{C_{F,m} - C_{D,b}\exp(-K \cdot J_w)}{1 - \left(\frac{B}{J_w}\right)[\exp(-K \cdot J_w) - 1]} \quad \text{(AL-FS mode)} \quad (9)$$

$$C_{F,m} = C_{D,m} - \frac{C_{D,m} - C_{F,b}\exp(K \cdot J_w)}{1 + \left(\frac{B}{J_w}\right)[\exp(K \cdot J_w) - 1]} \quad \text{(AL-DS mode)} \quad (10)$$

$$K = \frac{t\tau}{D\varepsilon} = \frac{S}{D} \quad (11)$$

where K is the salt resistivity to diffusion inside the porous support layer, S is the structure parameter, t, τ, and ε are the thickness, tortuosity, and porosity of the porous support layer, respectively.

For calculating water flux, the difference of effective osmotic pressure, which is described as the difference between $\pi_{F,m}$ and $\pi_{D,m}$, should be estimated. However, water flux should be necessary to calculate $C_{F,m}$ and $C_{D,m}$ in Eqs. (9) and (10). It means that the equations in the models are implicit, so the models should be solved

iteratively and numerically. In this study, one-dimensional mass balance equations were solved with an iterative procedure for ICP and ECP equations simultaneously until satisfying the tolerance. The mass balance equations of the FO process can be derived as follows [34]:

$$\frac{du_F}{dx} = -\frac{J_w}{H} \quad (12)$$

$$\frac{dC_F}{dx} = \frac{J_s + C_F J_w}{u_F H} \quad (13)$$

$$\frac{du_D}{dx} = \frac{J_w}{H} \quad (14)$$

$$\frac{dC_D}{dx} = \frac{-J_s - C_D J_w}{u_D H} \quad (15)$$

where u is the linear velocity and H is the channel height.

7. Parameter Estimation

We assumed the SW module can be modelled as large flat-sheet membrane module. Since the membrane material is CTA in both the FO SW and FO FS modules, the water permeability and salt permeability can be assumed as the same in both modules. Thus, the only influenced parameter according to the type of membrane module is the structure parameter. The membrane parameters such as A, B and S were already obtained from the reference [35]. From the S parameter in the reference, the new S parameter, which is appropriate to the FO SW module, was found by using parameter estimation with the experimental data from the FO SW module. The parameter estimation was carried out by using the built-in function "fminsearch" in MATLAB. The objective function was to minimize root mean square error between the experimental data and simulation results.

RESULTS AND DISCUSSION

1. Comparison of Water Flux in the FO SW and FO FS Modules

The water flux in the FO SW and FS modules was measured, respectively, as shown in Fig. 4. Fig. 4(a) shows the water flux values in the FO SW and FS modules at 0 mol/L (feed concentration) and 0.61 mol/L (draw concentration) as changing operating modes, and Fig. 4(b) at the conditions of 0.6 mol/L (feed concentration) and 1.21 mol/L (draw concentration). The feed and draw concentrations were designed to investigate how much the effect of concentration polarization would be severe as increasing the concentration of the feed and draw solutions while maintaining the bulk osmotic pressure difference. The water flux values in the FO SW module were always smaller than the FS FO module. Especially, the water flux in AL-DS mode in the FO SW module was significantly decreased from 8.464 L/m^{2}h to 3.093 L/m^{2}h with increasing the feed and draw concentrations, even though compared to any other results such as the flux in AL-FS mode and all of the results in the FO FS module. As increasing the feed and draw concentrations, the magnitudes of ECP and ICP increased, so the water flux was reduced. However, the reduction ratio in the FO SW module was higher than that in the FO FS module. It reveals that the magnitude of concentration polarization in the FO SW module

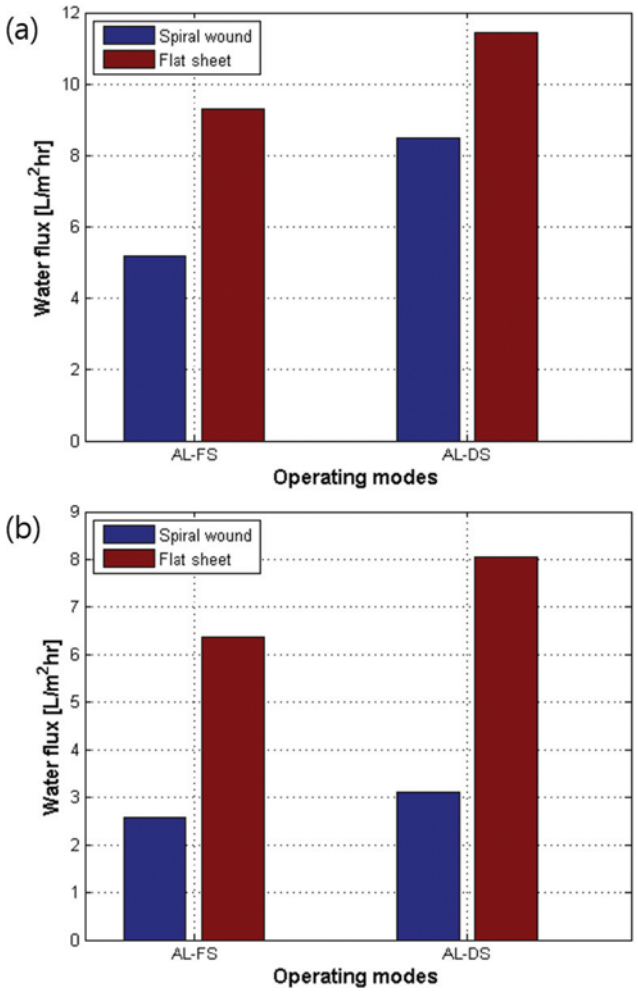

Fig. 4. (a) The water flux values from experimental results in the FO SW and FS modules at 0 M (feed concentration) and 0.61 M (draw concentration) as changing operating modes at 20-21 °C. (b) The water flux values from experimental results in the FO SW and FS modules at 0.6 M (feed concentration) and 1.21 M (draw concentration) as changing operating modes at 20-21 °C.

was much more severe than that in the FO FS module. It was also confirmed from the water flux in AL-DS mode. There was no ICP effect on the feed side in AL-DS mode when the feed concentration was 0 M in AL-DS mode, which is attributed to no concentration in the feed solution. When increasing the feed concentration from 0 mol/L to 0.6 mol/L, a significant reduction of water flux appeared due to the appearance of ICP on feed side. However, comparing the results in the FO SW and FO FS modules, the reduction of water flux in the FO SW module was considerably higher. From these results, it is concluded that the concentration polarization, especially ICP, highly occurred in the FO SW module than in the FO FS module. In addition, Table 1 shows the list of the water flux values from experimental results of the same FO SW module from other previous studies for comparison with the results in this study [26,27,32]. The water flux values from the experimental results of this study are comparable with the references. And, Table 2 shows the list of the water flux values from experimental

Table 1. The list of the water flux values from experimental results in the FO SW module with draw solution (NaCl) and feed solution (DI water) in operating modes (AL-FS and AL-DS) from other references

Operating mode	Concentration (mol/L)		Water flux (L/m^2h)	Temperature (°C)	References
	Draw solution (NaCl solution)	Feed solution (DI water)			
AL-FS	0.23	0	4.2	20	[27]
	0.44		7.1		
	0.66		9.3		
	0.85		10.9		
	0.5	0	4.7	20	[26]
	1.1		8.2		
	0.1	0	1.7	22-24	[32]
	0.3		3.6		
	0.5		5.8		
	0.8		6.4		
	0.61	0	5.16675	20-21	In this study
AL-DS	0.1	0	2.1	22-24	[32]
	0.3		4.6		
	0.5		6.2		
	0.8		8		
	0.61	0	8.46451	20-21	In this study

results of the same FO FS module from other previous studies, which are also comparable with our experimental data [16,29,35,36].

2. Parameter Estimation for the FO SW Model

Since the ICP effect in the FO SW module appears much higher than in the FO FS module, the previously reported FO membrane parameters from CTA membrane do not match with the FO SW module, even though the membrane material of the FO SW module is same as that of the FO FS module. As described in the previous section, the model for the FO SW module was developed as a large FS module, which has only different structure parameter from the FO FS module. To describe various conditions of feed and draw solution concentrations and to maintain the bulk osmotic pressure difference, the experimental conditions were designed as changing the feed concentration from 0 to 0.6 mol/L while maintaining the difference of concentration between draw solution and feed solution at the value of 0.61 mol/L.

Table 2. The list of the water flux values from experimental results in the FO FS module with draw solution (NaCl) and feed solution (DI water) in operating modes (AL-FS and AL-DS) from other references

Operating mode	Concentration (mol/L)		Water flux (L/m^2h)	Temperature (°C)	References
	Draw solution (NaCl solution)	Feed solution (DI water)			
AL-FS	0.25	0.01	5.6	22-24	[16]
	0.75		11.1		
	1.5		16.9		
	2		20.2		
	3		22.9		
	5.5		30		
	0.25	0	5	18	[29]
	0.5		6.2		
	0.7		7.5		
	0.9		8.6		
	1		9.4		
	1.5		11.2		
	5.25		17		
	0.5	0	7.8	25	[35]
	1.5	0	8.1	20	[36]
	0.61	0	9.273	20	In this study

Table 2. Continued

Operating mode	Concentration (mol/L)		Water flux (L/m^2h)	Temperature (°C)	References
	Draw solution (NaCl solution)	Feed solution (DI water)			
AL-DS	0.25	0.01	8.1	22-24	[16]
	0.5		17		
	0.75		21		
	1		28.2		
	1.5		34.2		
	2		43.3		
	3		48.3		
	4		55.7		
	0.5	0	13.4	25	[35]
	1.5	0	15.5	20	[36]
	0.61	0	11.42	20	In this study

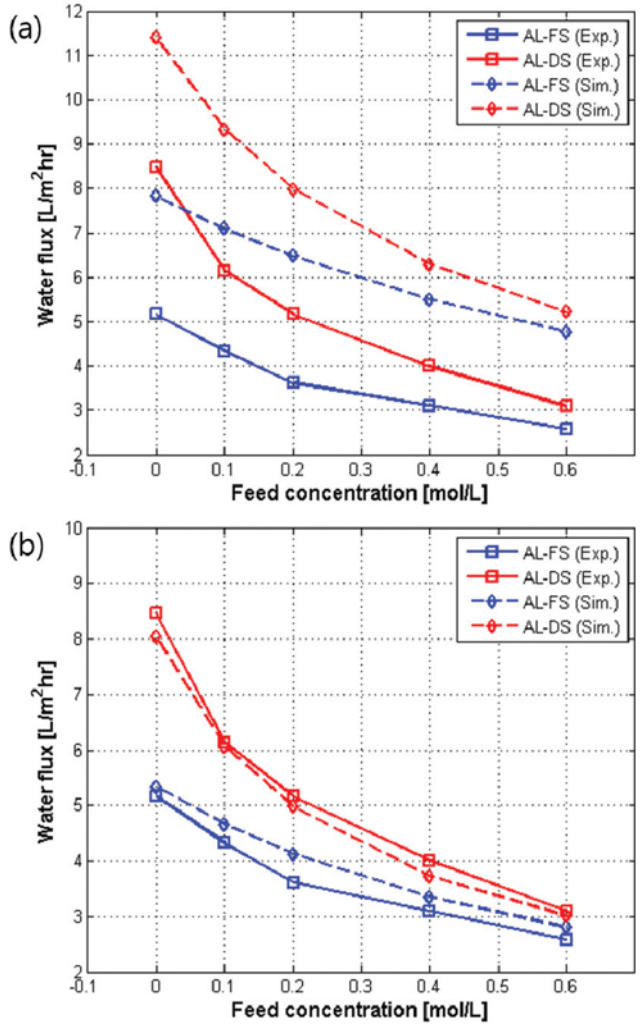

Fig. 5. (a) The water flux values from experimental results in the FO SW module and simulation results with the S parameter (4.20 ×10^{-4} m) as changing operating modes at 20-21 °C. (b) The water flux values from experimental results in the FO SW module and simulation results with the S parameter (9.1325× 10^{-4} m) with changing operating modes at 20-21 °C.

Fig. 5(a) shows the water flux values from experimental results in the FO SW module and simulation results with membrane parameters obtained from the FO FS module [35]. Although the membrane parameters properly describe the results in the FO FS module as previously reported [35], the parameters do not represent the flux behavior in the FO SW module appropriately. One of the reasons why full-scale module shows less water flux than lab-scale is that the full-scale membrane module would experience a reduction of driving force within the module itself because of the large amount of water permeation [36]. Even considering the driving force reduction in the simulation, the mismatch between experimental data and simulation results cannot be explained, as shown in Fig. 5(a). However, with changing membrane structure parameter as well as full-scale simulation, the experimental results could be appropriately described by a simulation approach. From parameter estimation, 9.1325×10^{-4} m was obtained as a structure parameter of the FO SW module. As shown in Fig. 5(b), the behavior of water flux in the FO SW module is represented by simulation quite appropriately, regardless of the concentrations and operating modes. It can be concluded that the model for the FO SW module can be easily formulated by just changing the structure parameter from the model for the FO FS module. Since a rigorous simulation for the FO SW module is quite difficult and requires very long computational time [33], this simple approach for the model of the FO SW module could be utilized effectively.

3. Validation of the FO SW Model from Different Draw Solutes

To validate the developed FO SW model, the water flux was measured by changing draw solutes, which were selected as draw solute candidates for operating hybrid FO, crystallization and RO process reported in our previous study [3]. The selected draw solutes were sodium sulfate (Na_2SO_4), and disodium phosphate (Na_2HPO_4), and were mixed with DI water. The test conditions of water flux measurement were the saturated concentrations of draw solutions of each draw solute (2.45 mol/L for Na_2SO_4 and 1.27 mol/L for Na_2HPO_4) and seawater concentration of feed solution (0.61 mol/L for NaCl). The temperature in each solution and experimental equipment was fixed at 30 °C. As the solubility of draw solutions is quite high and the ionization number is 3, the assumption that draw

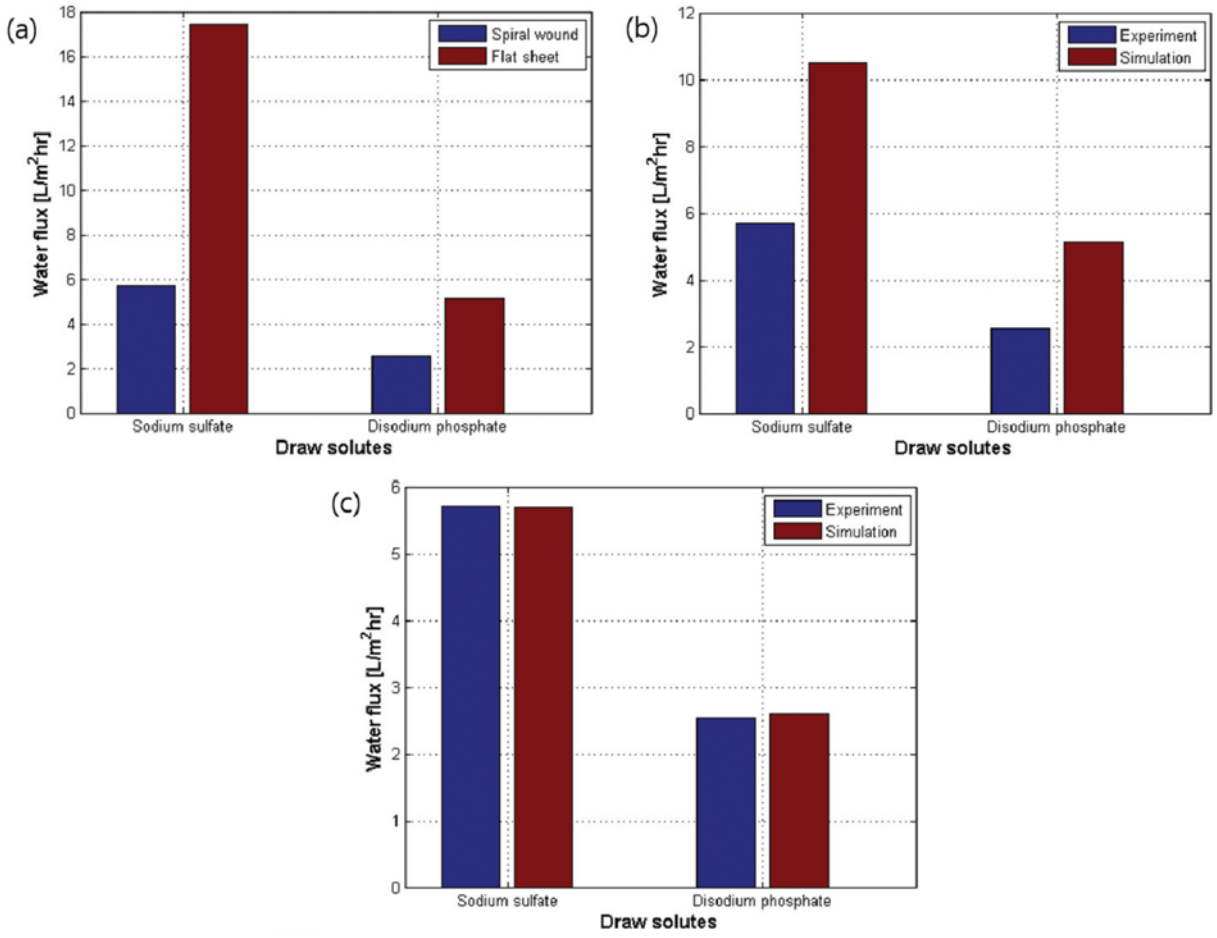

Fig. 6. (a) The water flux values from experimental results in the FO SW and FS modules with the saturated draw solutions at 30 °C. (b) The water flux values from experimental results in the FO SW module and simulation results with the S parameter (4.20×10^{-4} m) with the saturated draw solutions at 30 °C. (c) The water flux values from experimental results in the FO SW module and simulation results with the S parameter (9.1325×10^{-4} m) with the saturated draw solutions at 30 °C.

solutes were completely ionized in water would not be satisfied. In this study, the ionization numbers at each saturated draw solution were obtained from experiment with the FO FS module. The ionization number was determined as 2.3 in both sodium sulfate and disodium phosphate.

Fig. 6(a) shows the water flux values from experimental results in the FO SW and FS modules with each draw solution with saturation concentration at 30 °C. As in the previous section, the water flux values in the FO SW module were smaller than the FO FS module. The simulation results with membrane parameters of the FO FS module are shown in Fig. 6(b). The water flux from simulation with the FO FS module membrane parameters was overestimated compared to the experimental values. However, the simulation results with the FO SW module membrane parameters obtained from previous section estimate much accurate water flux as displayed in Fig. 6(c). The results imply that the developed FS SW model and

Table 3. The list of the water flux values from experimental results of the same FO SW module with different draw and feed solutions in AL-FS mode from other references

Operating mode	Concentration (mol/L)		Water flux (L/m^2h)	Temperature (°C)	References
	Draw solution	Feed solution			
AL-FS	NH_4HCO_3 (2 M) NH_4HCO_3 (3 M)+NH_4OH (2 M)	NaCl (0.55 M)	7.88 10.7	30	[27]
	$MgCl_2$ (0.5 M) $MgCl_2$ (1.1 M)	DI water (0 M)	5.4 8.9	20	[26]
	Na_2SO_4 (2.46 M) Na_2HPO_4 (1.27 M)	NaCl (0.61 M)	5.716 2.531	30-31	In this study

Table 4. The list of the water flux values from experimental results of the same FO FS module with different draw and feed solutions in AL-FS mode from other references

Operating mode	Concentration (mol/L)		Water flux (L/m^2h)	Temperature (°C)	References
	Draw solution	Feed solution			
AL-FS	NH_4HCO_3 (6 M)	NaCl (0.5 M)	22.9	50	[4]
	$MgCl_2$ (0.15 M)	DI water (0 M)	3.5	18	[29]
	$MgCl_2$ (0.4 M)		4.9		
	$MgCl_2$ (0.6 M)		5.5		
	$MgCl_2$ (0.8 M)		6.1		
	$MgCl_2$ (0.9 M)		7		
	$MgCl_2$ (1.4 M)		7.6		
	Na_2SO_4 (2.46 M) Na_2HPO_4 (1.27 M)	NaCl (0.61 M)	17.44057 5.1053	30	In this study

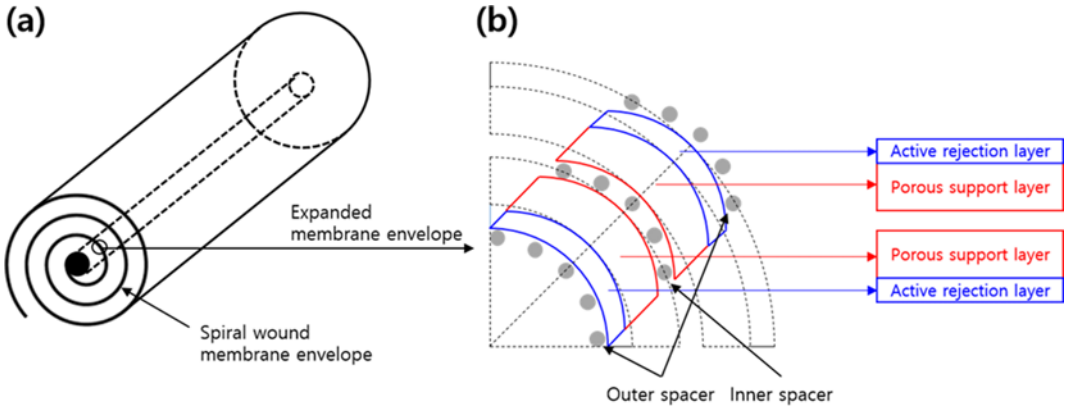

Fig. 7. (a) A cross-sectional view of the spiral wound membrane module loaded into a tubular vessel. (b) An expanded cross-sectional view of the membrane envelope.

estimated parameters could be applied even to other draw solutions. Tables 3 and 4 show the list of the water flux values from experimental results of the same FO SW and FO FS modules with different draw and feed solutions in AL-FS mode from other references [4,26,27,29]. The experimental results in this study are comparable to the other references.

4. Discussion about Changing Structure Parameter in the FO SW Module

Fig. 7(a) shows a cross-sectional view of the rolled FO SW membrane module loaded into a tubular vessel, and Fig. 7(b) shows an expanded cross-sectional view of the membrane envelope. To increase packing density of the SW module, the membrane envelopes are rolled around the central tube and loaded into the tubular vessels. This kind of structure is very effective for enhancing space utilization in full scale operation, but it is not suitable to the FO process. That's because the structure of the rolled membranes has different shape with the structure of flat membranes. As the membrane is bent in the SW module, the membrane support layer is shrunk and pressed as shown in Fig. 7. The inner pores of the membrane, especially in the porous support layer, are pressed and closed, and the membrane porous support layer thickness can be thicker as compared with the membrane support layer when the membrane was stretched out. In addition, since the membrane has more curves than before, the tortuosity related to the length of the curves becomes larger. Therefore, when the membrane is rolled, the membrane structure parameter value becomes larger, and the larger structure parameter also causes a reduction of the water flux. That's why the effect of the ICP appears high in the SW module compared to the FS module.

Even though the water flux reduction in the FO SW module can be explained by changing structure parameter, it is not the only reason for this phenomenon. Due to the complex structure in the FO SW module, the flow line in membrane envelopes is not simple. Thus, the FO SW module should be modelled by a very complex discretization procedure [33], or simulated by computation fluid dynamics (CFD) program with concerning the structure parameter change as well. However, this kind of approach is so complex that it cannot be easily implemented to estimate water flux in the FO SW module. In this study, all the effects which are attributed to the reduction of the water flux would be lumped into the estimated structure parameter. Although this kind of the lumped parameter approach does not estimate the water flux in the FO SW module based on the detailed simulation of all the effect, it could be successfully applied into the FO SW module for estimation of water flux with the satisfied accuracy. Moreover, the experimental results also revealed that the SW module is not suitable for the FO pro-

cess. Thus, a full scale module for the FO process should be designed with the direction not to bend the membrane, for example, plate and frame module.

CONCLUSIONS

The magnitude of internal concentration polarization in the FO SW membrane module was analyzed. Experiments in the FO SW membrane module and FO FS membrane module were conducted as changing operating modes and draw solutions. Experimental results were estimated by simulation results from the FO flux model. The water flux values in the FO SW module were smaller than the FS FO module from experimental results, regardless of the same and different feed and draw solutions. Even though the driving force reduction within the FO SW module was considered in the simulation, the water flux in the FO SW module could not be estimated. However, just by estimating new structure parameter (9.1325×10^{-4} m), all of the experimental data even with different draw solution (Na_2SO_4 and Na_2HPO_4) can be successfully estimated by the simple 1-D simulation approach. Since the structure parameter is affected by the porous support layer thickness, the tortuosity, and the porosity of the membrane, it can be concluded that the structure of the support layer would be changed as making the FO SW module. In the SW module, membrane envelopes are rolled around the central tube line, and the membrane support layer is bent. The flection causes the membrane porous support layer thickness to become larger, and the membrane porosity becomes smaller, which is attributed to the increase of the structure parameter. However, the membrane in the FS module is kept flat, so it does not seem to affect the support layer thickness, the tortuosity, and the porosity of the membrane. Therefore, to operate the FO process effectively, the FO membrane should not be bent like the SW module. Furthermore, a plate and frame module is recommended for the FO process since the module has higher active layer area compared to the SW module, and the larger capacity can be handled.

ACKNOWLEDGEMENTS

This work was financially supported by the Human Resources Development program (No. 20134010200600) of the Korea Institute of Energy Technology Evaluation and Planning (KETEP) grant funded by the Korea government Ministry of Trade, Industry and Energy, and Korea University grant.

REFERENCES

1. T. Y. Cath, A. E. Childress and M. Elimelech, *J. Membr. Sci.*, **281**, 70 (2006).
2. T.-S. Chung, S. Zhang, K. Y. Wang, J. Su and M. M. Ling, *Desalination*, **287**, 78 (2012).
3. D. Y. Kim, B. Gu, J. H. Kim and D. R. Yang, *J. Membr. Sci.*, **444**, 440 (2013).
4. J. R. McCutcheon, R. L. McGinnis and M. Elimelech, *Desalination*, **174**, 1 (2005).
5. D. L. Shaffer, N. Y. Yip, J. Gilron and M. Elimelech, *J. Membr. Sci.*, **415**, 1 (2012).
6. A. Achilli, T. Y. Cath, E. A. Marchand and A. E. Childress, *Desalination*, **239**, 10 (2009).
7. K. Lutchmiah, A. Verliefde, K. Roest, L. C. Rietveld and E. R. Cornelissen, *Water Res.*, **58**, 179 (2014).
8. J. Su, T.-S. Chung, B. J. Helmer and J. S. de Wit, *J. Membr. Sci.*, **396**, 92 (2012).
9. A. Achilli, T. Y. Cath and A. E. Childress, *J. Membr. Sci.*, **343**, 42 (2009).
10. Q. She, X. Jin and C. Y. Tang, *J. Membr. Sci.*, **401**, 262 (2012).
11. N. Y. Yip and M. Elimelech, *Environ. Sci. Technol.*, **46**, 5230 (2012).
12. X. Jin, J. Shan, C. Wang, J. Wei and C. Y. Tang, *J. Hazard. Mater.*, **227**, 55 (2012).
13. Q. Yang, K. Y. Wang and T.-S. Chung, *Sep. Purif. Technol.*, **69**, 269 (2009).
14. G. T. Gray, J. R. McCutcheon and M. Elimelech, *Desalination*, **197**, 1 (2006).
15. J. R. McCutcheon and M. Elimelech, *J. Membr. Sci.*, **284**, 237 (2006).
16. C. Y. Tang, Q. She, W. C. Lay, R. Wang and A. G. Fane, *J. Membr. Sci.*, **354**, 123 (2010).
17. S. Zhang, K. Y. Wang, T.-S. Chung, H. Chen, Y. Jean and G. Amy, *J. Membr. Sci.*, **360**, 522 (2010).
18. J. Wei, C. Qiu, C. Y. Tang, R. Wang and A. G. Fane, *J. Membr. Sci.*, **372**, 292 (2011).
19. P. G. Ingole and N. P. Ingole, *Korean J. Chem. Eng.*, **31**, 2109 (2014).
20. S. Loeb, L. Titelman, E. Korngold and J. Freiman, *J. Membr. Sci.*, **129**, 243 (1997).
21. J. T. Arena, B. McCloskey, B. D. Freeman and J. R. McCutcheon, *J. Membr. Sci.*, **375**, 55 (2011).
22. N.-N. Bui, M. L. Lind, E. M. Hoek and J. R. McCutcheon, *J. Membr. Sci.*, **385**, 10 (2011).
23. W. Fang, R. Wang, S. Chou, L. Setiawan and A. G. Fane, *J. Membr. Sci.*, **394**, 140 (2012).
24. S. S. Hong, W. Ryoo, M.-S. Chun and G.-Y. Chung, *Korean J. Chem. Eng.*, **32**, 1249 (2015).
25. C. Klaysom, T. Y. Cath, T. Depuydt and I. F. Vankelecom, *Chem. Soc. Rev.*, **42**, 6959 (2013).
26. E. Cornelissen, D. Harmsen, E. Beerendonk, J. Qin and J. Kappelhof, *J. Water Reuse Desalin.*, **1**, 133 (2011).
27. Y. C. Kim and S.-J. Park, *Environ. Sci. Technol.*, **45**, 7737 (2011).
28. A. Achilli, T. Y. Cath and A. E. Childress, *J. Membr. Sci.*, **364**, 233 (2010).
29. N. T. Hancock and T. Y. Cath, *Environ. Sci. Technol.*, **43**, 6769 (2009).
30. H. Y. Ng, W. Tang and W. S. Wong, *Environ. Sci. Technol.*, **40**, 2408 (2006).
31. J. E. Kim, S. Phuntsho, F. Lotfi and H. K. Shon, *Desalin. Water. Treat.*, **53**, 2782 (2015).
32. Y. Xu, X. Peng, C. Y. Tang, Q. S. Fu and S. Nie, *J. Membr. Sci.*, **348**, 298 (2010).
33. B. Gu, D. Kim, J. Kim and D. Yang, *J. Membr. Sci.*, **379**, 403 (2011).
34. D. Y. Kim, B. Gu and D. R. Yang, *Korean J. Chem. Eng.*, **30**, 1691 (2013).
35. S.-B. Kwon, J. S. Lee, S. J. Kwon, S.-T. Yun, S. Lee and J.-H. Lee, *J. Membr. Sci.*, **488**, 111 (2015).
36. L. Huang, N.-N. Bui, M. T. Meyering, T. J. Hamlin and J. R. McCutcheon, *J. Membr. Sci.*, **437**, 141 (2013).